

Pure

Scotland's Rural College

Use of the optical disector in canine mammary simple and complex carcinomas

Santos, M; Dias-Pereira, P; Correia-Gomes, C; Marcos, R; de Matos, A; Rocha, E; Lopes, C

Published in:

Acta Pathologica, Microbiologica et Immunologica Scandinavica (APMIS)

DOI:

[10.1111/apm.12717](https://doi.org/10.1111/apm.12717)

First published: 06/06/2017

Document Version

Peer reviewed version

[Link to publication](#)

Citation for pulished version (APA):

Santos, M., Dias-Pereira, P., Correia-Gomes, C., Marcos, R., de Matos, A., Rocha, E., & Lopes, C. (2017). Use of the optical disector in canine mammary simple and complex carcinomas. *Acta Pathologica, Microbiologica et Immunologica Scandinavica (APMIS)*, 125(9), 833 - 839. <https://doi.org/10.1111/apm.12717>

General rights

Copyright and moral rights for the publications made accessible in the public portal are retained by the authors and/or other copyright owners and it is a condition of accessing publications that users recognise and abide by the legal requirements associated with these rights.

- Users may download and print one copy of any publication from the public portal for the purpose of private study or research.
- You may not further distribute the material or use it for any profit-making activity or commercial gain
- You may freely distribute the URL identifying the publication in the public portal ?

Take down policy

If you believe that this document breaches copyright please contact us providing details, and we will remove access to the work immediately and investigate your claim.

1 **Use of the optical disector in canine mammary simple and complex carcinomas**

2 Marta Santos^{a,*}, Patrícia Dias-Pereira^b, Carla Correia-Gomes^c, Ricardo Marcos^a,
3 Augusto de Matos^{d,e}, Eduardo Rocha^{a,f}, Carlos Lopes^b

4

5 *^aDepartment of Microscopy, Laboratory of Histology and Embryology; ^bDepartment of*
6 *Pathology and Molecular Immunology; ^dDepartment of Veterinary Clinics, ICBAS –*
7 *UPorto, Portugal, Institute of Biomedical Sciences Abel Salazar, University of Porto,*
8 *ICBAS – UPorto, Portugal*

9 *^cEpidemiology Research Unit, Future Farming Systems, Scotland’s Rural College*
10 *(SRUC), Inverness, UK*

11 *^eAnimal Science and Study Central (CECA), Food and Agrarian Sciences and*
12 *Technologies Institute (ICETA)*

13 *^fHistomorphology, Physiopathology, and Applied Toxicology Group, Interdisciplinary*
14 *Centre for Marine and Environmental Research, CIIMAR – UPorto, Portugal*

15

16 * Corresponding author:

17 Marta Santos

18 Rua de Jorge Viterbo Ferreira, 228

19 4050-313 Porto, Portugal

20 Tel.: +351220428243

21 E-mail address: mssantos@icbas.up.pt

22 Running title: Numerical density in canine mammary tumors

23 **Summary**

24 Grading of canine mammary carcinomas (CMC) is associated to subjective assessments
25 made by the pathologists. Due to its unbiased nature, stereology can be used to
26 objectively quantify morphological parameters associated with grading and malignancy.
27 However, the use of stereology in CMC has not been fully disclosed. The nuclear
28 numerical density [N_V (nuclei, tumor)] is a cellularity-associated parameter that can be
29 estimated by the optical disector. Herein, it was estimated in 44 CMC and its
30 association with clinicopathologic factors — such as tumor size, histological subtype
31 and grade, vascular/lymph node invasion, nuclear pleomorphism and survival — was
32 evaluated. Considering all the cases, the mean N_V (nuclei, tumor) was $1.6 \times 10^6 \pm$
33 0.5×10^6 nuclei mm^{-3} . Lower values were attained in complex carcinomas, comparing to
34 simple carcinomas, in tumors smaller than 5 cm, with low mitotic activity and in those
35 with high nuclear pleomorphism. No statistically significant association with grade or
36 vascular/lymph node invasion was observed, but tumors with disease progression had
37 lower nuclear densities. The N_V (nuclei, tumor) and the correlated parameters mirror to
38 some extension those in human breast cancer, suggesting an interesting interspecies
39 agreement. This first estimation of the nuclear numerical density in CMC highlights the
40 feasibility of the optical disector and their utility for objective morphological
41 assessments in CMC. The association between nuclear numerical density and disease
42 progression warrants future studies.

43

44 **Keywords:** canine mammary tumors; disector; grade; prognosis; stereology

45 **Introduction**

46 The level of knowledge in canine mammary carcinomas (CMC) has increased
47 considerably in recent years, with various putative prognostic factors been pointed (1).
48 However, it is still recognized that the marked clinical and morphological heterogeneity,
49 including the possibility of multiple synchronous CMC of different subtypes could
50 make the assessment of the prognosis difficult (2). Moreover, the different
51 methodological approaches and end-points used in prognostic studies of CMC puzzled
52 the identification of definitive prognostic factors (2).

53 Despite the development of sophisticated “omics” technologies in oncology, tumor
54 morphology continues to be a powerful mode of providing clinical and prognostic
55 informative data (3). Still, it is recognized that the histopathological assessment of
56 tumor features is not entirely objective and this can jeopardize the biological
57 conclusions, namely in terms of prognosis (4). Such subjectivity may be overcome by
58 quantitative morphological parameters assessed by suitable morphometric or
59 stereological methods (5, 6). These methods are substantially different: while
60 morphometry describes quantitatively what is seen in conventional sections [under the
61 microscope or in two-dimensional (2D) images], using a caliper and sometimes
62 benefiting from image-analysis software, stereology uses probes or test-systems in 2D
63 images or virtual optical z-planes, aiming to obtain three-dimensional (3D) information
64 inherent of all biological tissues (5-7). Stereology can be used in histological sections of
65 tumors, allowing unbiased estimates (in relation to the 3D reality) of many parameters,
66 such as absolute or relative volumes of the cells or their nuclei and numerical nuclear
67 densities (4, 8).

68 Stereological studies have been performed in human breast cancer and estimates of
69 nuclear volumes (volume and number-weighted mean nuclear volumes) and of

70 numerical density (N_V) of nuclei and mitotic figures have been correlated with
71 prognosis (4, 8-10). In CMC, the use of stereology is still very incipient (11), but it
72 already started to solve issues related with the subjective assessment of nuclear
73 pleomorphism in grading of CMC (12).

74 CMC are classified according to the cell populations presented within the tumor, as
75 simple (one neoplastic cell population, epithelial or myoepithelial of origin) or complex
76 (when epithelial and myoepithelial cells coexist) (13). In simple carcinomas, the
77 architectural arrangement of the neoplastic epithelial cells, e.g., the presence of
78 tubulopapillary structures or solid sheets is included in the histological classification,
79 with some special subtypes such as squamous cell or mucinous carcinomas being
80 characterized by specific morphological features (13).

81 It has been suggested that highly cellular CMC, *i.e.* solid subtypes, are associated with a
82 poorer prognosis compared with tubulopapillary tumors (13, 14). However, cellularity
83 assessed by pathologists tends to be qualitative and may be subjective. To the best of
84 our knowledge, a quantitative evaluation of a cellularity parameter, such as the N_V , has
85 never been performed in CMC. Such an evaluation can be performed by the optical
86 disector (7, 15). Instead of counting nuclear cell profiles, which not only depend on the
87 cell number but also on the size, shape, and spatial orientation and distribution of nuclei,
88 the disector uses a 3D counting cube with inclusion and exclusion sides that allows
89 counting nuclei in proportion to their real number (5, 6, 16).

90 The primary aims of this study were to estimate the N_V (nuclei, tumor) in CMC and
91 their relation with other clinicopathological parameters, namely tumor size, histological
92 subtype, vascular/lymph node invasion and histological grading parameters (*i.e.* tubule
93 formation, nuclear pleomorphism and mitotic count). Ultimately we intended to
94 evaluate the prognostic utility of the N_V (nuclei, tumor) in CMC.

95 **Materials and Methods**

96 *Selection of cases and histological analysis*

97 Forty four spontaneous CMC treated at UPvet (Veterinary Hospital of the University of
98 Porto) were retrospectively selected, blinded to clinical and other pathological data. The
99 female dogs were submitted to surgical resection of the tumors with the owner's
100 consent. For twenty seven cases follow-up data were collected prospectively over two
101 years following a protocol detailed elsewhere (2). The histological diagnosis and
102 grading was reviewed by two pathologists (MS and PDP) using the criteria of the World
103 Health Organization classification (17) and the Nottingham histological grade (NHG)
104 (18). For this, routine 5 µm sections resulting from the largest cross slab of the tumor
105 were retrieved and screened. For every case, the tumor size and the histological
106 evidence of vascular invasion and/or regional lymph node metastases were recorded. As
107 to tumor size, it was categorized according to World Health Organization (WHO)
108 criteria (T1< 3 cm, T2=3-5 cm and T3> 5 cm), as previously described (19).

109

110 *Sectioning and stereological analysis*

111 For every case, a thick section (30 µm thick) from all the paraffin blocks was obtained.
112 To avoid chatter, the surface of the paraffin block was warmed (by breathing on)
113 immediately before cutting. After being picked from the water-bath, the sections were
114 covered with a cotton cloth and gently pressed against the slide with a finger, for
115 ensuring adhesion. All the sections were mounted on precleaned slides primed with
116 aminopropyltriethoxy-silane. Finally, sections were dried overnight at 37°C and then
117 stained with hematoxylin-eosin.

118 For the stereological analysis we used a workstation comprising: 1) a microscope
119 (Olympus BX-50, Tokyo, Japan) equipped with a 100x oil-immersion lens (Olympus

120 Uplan NA = 1.35, Tokyo, Japan) and a matching condenser; 2) a microcator
121 (Heidenhain MT-12, Traument, Germany), to control the movements and position in
122 the z-direction (0.5 μm accuracy); 3) a motorized stage (Prior, Fulbourn, United
123 Kingdom) for stepwise displacement in the x–y directions (1 μm accuracy); 4) a CCD
124 video camera (Sony, Tokyo, Japan) connected to a 17" PC monitor (Sony); and 5) a
125 computer with a stereology software (Olympus CAST-Grid, version 1.5, Albertslund,
126 Denmark). At the monitor, a final magnification of 4750x allowed an accurate
127 recognition of the nuclei of the neoplastic cells. The first field of vision was randomly
128 selected by the software. Thereafter, fields were sampled systematically by stepwise
129 movements of the stage in the x- and y-directions, so that a minimum of 40 fields were
130 examined per tumor. Throughout the disector height ($h = 16 \mu\text{m}$), a software generated
131 counting frame was superimposed, having a defined area of $253 \mu\text{m}^2$ and inclusion and
132 forbidden lines (Fig. 1), to prevent the edge effect counting bias (20).

133 Nuclei were counted when two conditions were met: (1) at the plane of focus, they were
134 within the counting frame or touching the inclusion lines and not touching the forbidden
135 lines or their extensions; (2) the rim of the nucleus was in perfect focus at a plane below
136 $4 \mu\text{m}$ and above or equal to $20 \mu\text{m}$ in the z-axis (Fig. 1). The potential bias from lost
137 caps was avoided by an upper guard height ($4 \mu\text{m}$) and a lower one (from $20 \mu\text{m}$
138 downward) (5). Spindle-shaped nuclei were excluded from the counts.

139 The N_V (nuclei, tumor) was estimated using the formula (21):

$$140 \quad N_V(\text{nuclei, tumor}) = \Sigma Q^- / [h \times a(\text{frame}) \times \Sigma P]$$

141 where ΣQ^- corresponded to the sum of neoplastic nuclei counted in the sampled fields,
142 and $a(\text{frame})$, h and ΣP were, respectively, the area of the counting frame, disector
143 height and the total number sampled fields within the reference space. Since the
144 reference space defined was the parenchyma of the tumor, fields that were empty,

145 containing large vessels, stroma, or necrotic areas were excluded. The coefficient of
146 error (CE) of the estimations of N_V (nuclei, tumor) was determined using the formula
147 (16):

$$148 \quad CE(N_V) = \sqrt{\frac{\Sigma u^2}{\Sigma u \cdot \Sigma u} + \frac{\Sigma v^2}{\Sigma v \cdot \Sigma v} - 2 \frac{\Sigma u \cdot v}{\Sigma u \cdot \Sigma v}}$$

149 where u and v stands for the number of nuclei counted (Q) and total number sampled
150 fields within the reference space (P), respectively.

151 The CE of the N_V estimations was then compared with the observed relative variance
152 among cases, OCV^2 , according to the formula (16):

$$153 \quad OCV^2 = BCV^2 + CE^2(N_V)$$

154 where BCV^2 is the inherent biological relative variance of the N_V in tumors and CE^2 is
155 the mean square of the individual estimates of the CE of N_V .

156

157 *Shrinkage estimation*

158 It would be reasonable to assume that the shrinkage in x-y would be alike in all the
159 included cases, as they were handled by the same surgical team and submitted to similar
160 processing protocols. Despite this, estimation of the shrinkage in thick sections of each
161 case was performed. For this, blood vessels were randomly photographed and the
162 erythrocyte diameter was measured in 30 cells (measurements were restricted to
163 erythrocytes appearing as clear circles). It should be stressed that: 1) animals had no
164 hematological abnormality in their pre-surgical evaluation; and 2) a diameter of 7.0 μm
165 was considered for normal canine erythrocytes (22).

166

167 *Statistical analysis*

168 To test if the data followed a normal distribution the Shapiro-Wilk and Kolmogorov-
169 Smirnov tests were used. For skewed data, a logarithmic transformation was applied.

170 The associations between the N_V (nuclei, tumor) and: 1) NHG grade (grade I, II and III);
171 2) grading parameters — tubule formation, nuclear pleomorphism and mitotic counts
172 scores; 3) WHO size categories; and 4) histological subtypes, were tested with one-way
173 ANOVA, followed by Tukey post-hoc tests. The association degree between the N_V
174 (nuclei, tumor) and the volume-weighted mean nuclear volume [previously assessed by
175 point sampled intercepts (12)] was evaluated by Pearson correlation test. In all cases, a
176 P value < 0.05 was considered significant. Statistical analyses were performed with the
177 IBM SPSS Statistics, version 22 (IBM, New York, USA).

178 **Results**

179 Thirty out of 44 tumors were diagnosed as simple carcinomas (11 tubulopapillary, 16
180 solid, 2 squamous cell and 1 mucinous) and 14 were complex carcinomas. At the time
181 of diagnosis, 12 cases (27%) presented vascular/regional lymph node invasion. With
182 regard to NHG, 9, 15 and 20 cases were grade I, II and III, respectively. Follow-up data
183 were available for 27 female dogs and during this period 30% (8/27) presented
184 progression of the disease (defined as recurrence and/or metastases *de novo*). Of the
185 remaining, 56% (15/27) were alive and clinically disease-free at 24 months after the
186 surgery, whilst 14% (4/27) were censored for being lost to follow-up or for non-
187 malignancy-related death. The clinicopathological parameters are summarized in Table 1.
188 The optical disector procedure was straightforward. Sections had a mean thickness of
189 $28.9 \pm 2.8 \mu\text{m}$ and around 6 cells nuclei were computed *per* disector. In average, 259
190 nuclei *per* tumor were counted and the N_V (nuclei, tumor) was estimated as $1.6 \times 10^6 \pm$
191 0.5×10^6 nuclei mm^{-3} (Fig.2). The mean CE of the N_V (nuclei, tumor) estimations was
192 0.07 (ranged from 0.04 to 0.11), meaning that the estimation methodology was
193 responsible for 5% of the total observed variance. Therefore, the biological variability
194 was by far the most important component of the observed variability of the N_V (nuclei,
195 tumor) estimations.

196 The N_V (nuclei, tumor) was significantly higher in simple carcinomas ($1.7 \times 10^6 \pm$
197 0.5×10^6 nuclei mm^{-3}) comparing with complex carcinomas ($1.3 \times 10^6 \pm 0.2 \times 10^6$ nuclei
198 mm^{-3}) (t-test, $P = 0.002$). No statistical difference was observed when solid carcinomas
199 were compared with any other subtypes. The N_V (nuclei, tumor) was 1.3×10^6 , 1.7×10^6
200 and 1.6×10^6 nuclei mm^{-3} in grade I, II, III tumors, respectively, without statistically
201 significant differences. With regard to NHG parameters, the N_V (nuclei, tumor) did not
202 differ with the tubule formation score, but an association with nuclear pleomorphism

203 was observed — tumors scored 3 for nuclear pleomorphism presented lower N_V (nuclei,
204 tumor) compared to tumors scored 2 (Tukey test, $P = 0.021$). Similarly, a statistically
205 significant increase in numerical nuclear density existed from tumors scored 1 or 2 to
206 those scored 3 in mitotic counts (Tukey test, $P = 0.006$ score 1 *versus* score 3 and P
207 $= 0.013$ score 2 *versus* score 3). With respect to tumor size, no difference in N_V (nuclei,
208 tumor) was observed in tumors of each the three WHO size category. However, when
209 tumors larger than 5 cm were compared with smaller tumors, the first ones presented a
210 significant higher N_V (nuclei, tumor) (t -test, $P = 0.030$).

211 The N_V (nuclei, tumor) was weak-to-moderately correlated with the volume-weighted
212 mean nuclear volume ($r = -0.34$; $P = 0.027$) — *i.e.* the N_V (nuclei, tumor) tended to be
213 lower in tumors presenting higher nuclear pleomorphism.

214 As to vascular/lymph node invasion status, the N_V (nuclei, tumor) was similar in tumors
215 with and without evidence of invasion. In the same line, no significant association
216 between the N_V (nuclei, tumor) and the post-surgical disease progression was detected.
217 However, the eight cases that showed post-surgical disease progression during the
218 follow-up period presented a lower N_V (nuclei, tumor) (1.4×10^6 nuclei mm^{-3}) when
219 compared with cases without evidence of metastases and/or recurrence (1.8×10^6 nuclei
220 mm^{-3}) (t -test, $P = 0.047$).

221 The estimated shrinkage in x - y was $35.8\% \pm 2.3\%$, with no significant differences
222 between cases.

223 **Discussion**

224 Studies over the last thirty years have built a consensus on the value of quantification
225 for improving the prognostic value of morphological parameters in malignant tumors (9,
226 23-28). Stereological methods not only achieve such quantification, but have additional
227 advantages of unbiasedness and reproducibility (5, 6). These have been applied for long
228 in breast pathology (8, 27), but their use in the veterinary oncology is still incipient (11).
229 Herein, the optical disector was used to assess the N_V (nuclei, tumor) in CMC. Notably,
230 the mean value for CMC (1.6×10^6 nuclei mm^{-3}) was higher (but in the same order of
231 magnitude) than that reported for human breast cancer (0.4×10^6 nuclei mm^{-3}) (10).
232 Interspecies differences may underlie such discrepancy, along with eventual technical
233 discrepancies, particularly in the definition of the reference space (for example, we
234 excluded stromal areas). Still, our data suggest that CMC present a higher numerical
235 density of nuclei than human breast carcinomas. Despite the differences in figures
236 between our and human studies, some observations in breast cancers were mirrored to
237 some extension in CMC. For instance, there was no significant association between N_V
238 (nuclei, tumor) and histological grade, but a significant negative correlation was noted
239 between the N_V (nuclei, tumor) and the volume-weighted mean nuclear volume — $r = -$
240 0.34, -0.63 and -0.31 in our study and in the two existing breast cancer estimations
241 [respectively, (10) and (27)].

242 Another interesting finding in both species is that cancers with worst survival outcomes
243 presented a lower N_V (nuclei, tumor) (10). At a first glance, this is an unexpected
244 observation that appears to contradict the traditional concept that highly cellular tumors
245 are associated with poorer prognosis (13). However, it should be kept in mind that any
246 numerical density is a relative parameter (*i.e.* a fraction) that can be influenced by the
247 number of nuclei/cells or by changes in the reference space (*i.e.* decreases in numerator

248 or increases in the denominator). A decrease in the N_V (nuclei, tumor) can occur in
249 different scenarios, namely when cells get larger, or appear more distant (*e.g.* either due
250 to an increase in extracellular matrix, as it probably occurs in complex carcinomas, or
251 due to the loss of epithelial adhesion), or when an increased nuclear/cellular
252 pleomorphism exists (Fig.3). The latter is more likely to occur in CMC, since it was
253 previously described that the volume-weighted mean nuclear volume was significantly
254 higher in more aggressive tumors (12), and herein a negative correlation between the
255 nuclear volume parameter and the N_V (nuclei, tumor) existed.

256 Herein the N_V (nuclei, tumor) did not differ between solid and tubulopapillary
257 carcinomas. This supports that the presence of luminal structures in routine sections is
258 not directly correlated with cellularity at 3D level. According to the present data, both
259 solid and tubulopapillary carcinomas are heterogeneous regarding the 3D densities of
260 nuclei, which is in accordance to previous studies describing variability in those
261 subtypes of tumors using immunohistochemistry (*e.g.* 29). Yet, this study evidenced
262 that complex carcinomas have decreased N_V (nuclei, tumor). A possible explanation for
263 this could reside in the presence of small portions of myxoid matrix, typical of these
264 tumors (13). When being surrounded by that extracellular matrix, cells tend to appear
265 separated and, thus fewer neoplastic cell nuclei would be counted in the disector (Fig.
266 3C).

267 Paraffin shrinkage during tissue processing can influence the reference space and,
268 therefore, lead to overestimations of the N_V (5, 30). In this study, the shrinkage was
269 similar to that reported for thick paraffin sections (30, 31). In this case, the overall N_V
270 (nuclei, tumor) corrected for shrinkage would be $1.17 \times 10^6 \pm 0.5 \times 10^6$ nuclei mm^{-3} .
271 Theoretically, problems arise by comparing estimations of tissues with different
272 amounts of shrinkage. This is unlikely to have influenced our results, not only because

273 all the cases were handled and processed similarly, but also because no significant
274 differences in the diameter of erythrocytes between cases were noted. In fact, it should
275 be stressed that the possibility of bias related to tissue handling when stereology is
276 applied to routine diagnostic material should never cloud the advantages of stereology
277 over traditional 2D techniques (32). These latter are not only affected by shrinkage, but
278 are also severely influenced (in an uncontrolled extent) by the shape, orientation and
279 size of the particles being counted (6, 16, 30).

280 As a final methodological appraisal, in this first approach to the N_V (nuclei, tumor) of
281 CMC we obtained a small CE, much below the 0.1 threshold (16), and the error due to
282 the methodology was low. For future studies and for practical purposes, the CE could be
283 optimized, by counting fewer nuclei per tumor. In this vein, counting 20 fields per
284 tumor would suffice and this would significantly reduce the time needed for the analysis
285 (for forty fields, around 30 minutes were needed).

286 Spontaneous CMC have been pointed as a suitable model for human breast cancer,
287 based on similarities in epidemiological data, risk factors, molecular characteristics, and
288 clinical course of the disease (e.g. 33, 34). The subtypes of simple CMC are more
289 similar, in terms of the histological features, to the most frequent human breast
290 carcinomas. The quantitative data presented herein strengthened the similarity of those
291 canine tumors with human breast carcinomas.

292

293 **Conclusion**

294 We showed in CMC that an unbiased and reproducible estimation of a cellularity-related
295 parameter — expressed as N_V (nuclei, tumor) — can be obtained by stereological
296 methods. The mean N_V (nuclei, tumor) was lower in complex carcinomas, in smaller
297 tumors, and in those with low mitotic activity and high nuclear pleomorphism. No

298 association with vascular/lymph node invasion was observed, but nuclear numerical
299 density was lower in cases that progressed during follow-up. This association is a
300 promising finding, suggesting that the N_V (nuclei, tumor) have potential to be used to
301 assess survival outcome in CMC. For this, further and larger studies are required.

302

303 **Acknowledgments**

304 The authors thank Fernanda Malhão and Célia Lopes (ICBAS-UP, University of Porto)
305 for their technical support in preparing the thick sections.

306

307 **References**

308 1 Sleecx N, de Rooster H, Kroeze EJBV, Van Ginneken C, Van Brantegen L. Canine
309 mammary tumours, an overview. *Reprod Domest Anim* 2011; 46:1112-31.

310

311 2 Matos AJ, Baptista CS, Gärtner MF, Rutteman GR. Prognostic studies of canine and
312 feline mammary tumours: the need for standardized procedures. *Vet J* 2012; 193:24-31.

313

314 3 Lakhani SR, Reis-Filho JS, van de Vijver MJ. Molecular pathology overview. In:
315 WHO classification of tumors of the breast. SR Lakhani, IO Ellis, SJ Schnitt, PH Tan,
316 MJ van der Vijver, editors. Lyon: IARC, 2012:28.

317

318 4 Sørensen FB. Quantitative analysis of nuclear size for objective malignancy grading: a
319 review with emphasis on new, unbiased stereologic methods. *Lab Invest* 1992; 66:4-23.

320

321 5 Marcos R, Monteiro RA, Rocha E. The use of design-based stereology to evaluate
322 volumes and numbers in the liver: a review with practical guidelines. *J Anat* 2012;
323 220:303-17.

324

325 6 Geuna S, Herrera-Rincon C. Update on stereology for light microscopy. *Cell Tissue*
326 *Res* 2015; 360:5-12.

327

328 7 Geuna S. Appreciating the difference between design-based and model-based
329 sampling strategies in quantitative morphology of the nervous system. *J Comp Neurol*
330 2000; 427:333-9.

331

332 8 Ladekarl M. Objective malignancy grading: a review emphasizing unbiased
333 stereology applied to breast tumors. *APMIS Suppl* 1998; 79:1-34.

334

335 9 Ladekarl M, Sørensen FB. Quantitative histopathological variables in in situ and
336 invasive ductal and lobular carcinomas of the breast. *APMIS* 1993; 101:895-903.

337

- 338 10 Artacho-Pérula E, Roldán-Villalobos R. Unbiased stereological estimation of the
339 number and volume of nuclei and nuclear size variability in invasive ductal breast
340 carcinomas. *J Microsc* 1997; 186:133-42.
341
- 342 11 Casteleyn C, Prims S, Van Cruchten C. Stereology: from astronomy to veterinary
343 oncology. *Vet J* 2014; 202:3-4.
344
- 345 12 Santos M, Correia-Gomes C, Santos A, de Matos A, Rocha E, Lopes C, Pereira PD.
346 Nuclear pleomorphism: role in grading and prognosis of canine mammary carcinomas.
347 *Vet J* 2014; 200:426-33.
348
- 349 13 Misdorp W. Tumors of the mammary gland. In: *Tumors of Domestic Animals*, 4th
350 Edition, DJ Meuten, editor, Iowa: Iowa State Press, 2002:575-606.
351
- 352 14 Sorenmo K. Canine mammary gland tumors. *Vet Clin North Am Small Anim Pract*
353 2003; 33:573-96.
354
- 355 15 Sterio DC. The unbiased estimation of number and sizes of arbitrary particles using
356 the disector. *J Microsc* 1984; 134:127-36.
357
- 358 16 Gundersen HJG, Miabile R, Brown D, Boyce RW. Stereological principles and
359 sampling procedures for toxicologic pathologists. In: *Haschek and Rousseaux's*
360 *Handbook of Toxicologic Pathology*. WN Haschek, CG Rousseaux, MA Walling,
361 editors. Waltham: Elsevier Inc., Academic Press, 2013: 215-86.
362
- 363 17 Misdorp W, Else RW, Hellmén E, Lipscomb TP. Histological classification of
364 mammary tumors of the dog and the cat, 2nd series. In: *World Health Organization*
365 *International Histological Classification of Tumours of Domestic Animals*, volume VII,
366 Washington: Armed Forces Institute of Pathology, 1999.
367
- 368 18 Elston CW, Ellis IO. Pathological prognostic factors in breast cancer. I. The value of
369 histological grade in breast cancer: experience from a large study with long-term
370 follow-up. *Histopathology* 1991; 19:403-10.
371
- 372 19 Owen LN. Classification of tumors in domestic animals. Geneva:World Health
373 Organization:1-54.
374
- 375 20 Gundersen HJG. Notes on the estimation of numerical density of arbitrary particles:
376 the edge effect. *J Microsc* 1977; 111:219-23.
377
- 378 21 Gundersen HJ, Bagger P, Bendtsen TF, Evans SM, Korbo L, Marcussen N, et al. The
379 new stereological tools: disector, fractionator, nucleator and point sampled intercepts
380 and their use in pathological research and diagnosis. *APMIS* 1988; 96:857-81.
381
- 382 22 Reece WO. The composition and functions of blood. In: *Duke's physiology of*
383 *domestic animals*. 13th edition, Reece WO, editor. Iowa: John Willey & Sons Inc. Ames,
384 2015:114-36.
385
- 386 23 Baak JPA, Von Dop H, Kurver PHJ, Hermans J. The value of morphometry to
387 classic prognosticators in breast cancer. *Cancer* 1985; 56:374-82.

388
389 24 van der Linden HC, Baak JPA, Lindeman J, Hermans J, Meyer CJLM. Morphometry
390 and breast cancer II. Characterization of breast cancer cells with high malignant
391 potential in patients with spread to lymph nodes: preliminary results. *J Clin Pathol*
392 1986; 39:603-09.
393
394 25 Ladekarl M, Sørensen FB. Prognostic, quantitative histopathologic variables in
395 lobular carcinoma of the breast. *Cancer* 1993; 72:2602-11.
396
397 26 Ladekarl M. Quantitative histopathology in ductal carcinoma of the breast.
398 Prognostic value of mean nuclear size and mitotic counts. *Cancer* 1995; 75:2114-22.
399
400 27 Ladekarl M. Choice of methodology for quantifying cancer structures in tissue
401 sections. A comparison of 2- and 3-dimensional estimators of mitotic activity,
402 cellularity and nuclear size in breast cancer. *Anal Quant Cytol Histol* 2004; 26:97-104.
403
404 28 Nedergaard BS, Nielsen K, Nyengaard JR, Ladekarl M. Stereologic estimation of the
405 total numbers, the composition and the anatomic distribution of lymphocytes in cone
406 biopsies from patients with stage I squamous cell carcinoma of the cervix uteri. *APMIS*
407 2007; 115:1321-30.
408
409 29 Yoshimura H, Nakahira R, Kishimoto TE, Michishita M, Ohkusu-Tsukada K,
410 Takahashi K. Differences in indicators of malignancy between luminal epithelial cell
411 type and myoepithelial cell type of simple solid carcinoma in the canine mammary
412 gland. *Vet Pathol* 2014; 51:1090-95.
413
414 30 Mandarim-Lacerda CA. Stereological tools in biomedical research. *An Acad Braz*
415 *Cienc* 2003; 75:469-86.
416
417 31 Salisbury JR. Three-dimensional reconstruction in microscopical morphology. *Histol*
418 *Histopathol* 1994; 9:773-80.
419
420 32 Kamp S, Jemec GB, Kemp K, Kjeldsen CR, Stenderup K, Pakkenberg B, et al.
421 Application of stereology to dermatological research. *Exp Dermatol* 2009; 18:1001-09.
422
423 33 Klopfleisch R, Lenze D, Hummel M, Gruber AD. Metastatic canine mammary
424 carcinomas can be identified by a gene expression profile that partly overlaps with
425 human breast cancer profiles. *BMC Cancer* 2010; 10:618.
426
427 34 Queiroga FL, Raposo T, Carvalho MI, Prada J, Pires I. Canine mammary tumours as
428 a model to study human breast cancer: most recent findings. *In Vivo* 2011; 25:455-65.
429
430
431
432

	Simple carcinomas (<i>n</i> =30)			Complex carcinomas
	Tubulopapillary (<i>n</i> =11)	Solid (<i>n</i> =16)	Others (<i>n</i> =3)	(<i>n</i> =14)
N_V (nuclei, tumor) (mean, μm)	1.8×10^6	1.7×10^6	1.6×10^6	1.3×10^6
Tumor size <3 cm	10	5	1	9
Tumor size 3-5 cm	0	4	1	2
Tumor size > 5 cm	1	7	1	3
Histological grade I	2	0	0	7
Histological grade II	7	3	1	4
Histological grade III	2	13	2	3
Vascular/lymph node invasion	2	8	0	2
Disease progression (recurrence and/or metastasis)*	1	5	0	2

*Follow up data was available for 22 cases with simple carcinomas and 5 cases with complex carcinomas

434

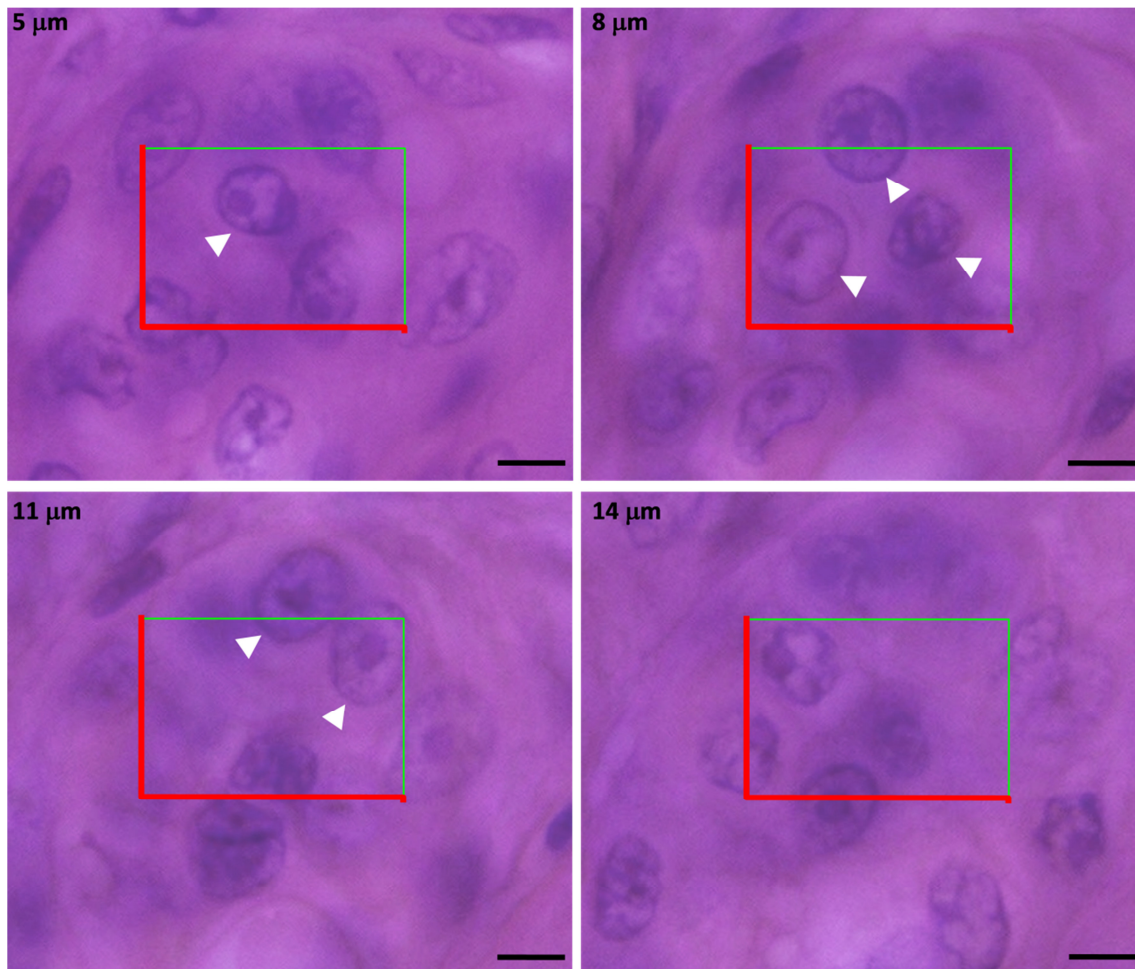
435

436

Table 1: Numerical nuclear density and relevant clinicopathological parameters of the 44 canine mammary carcinomas used in this study.

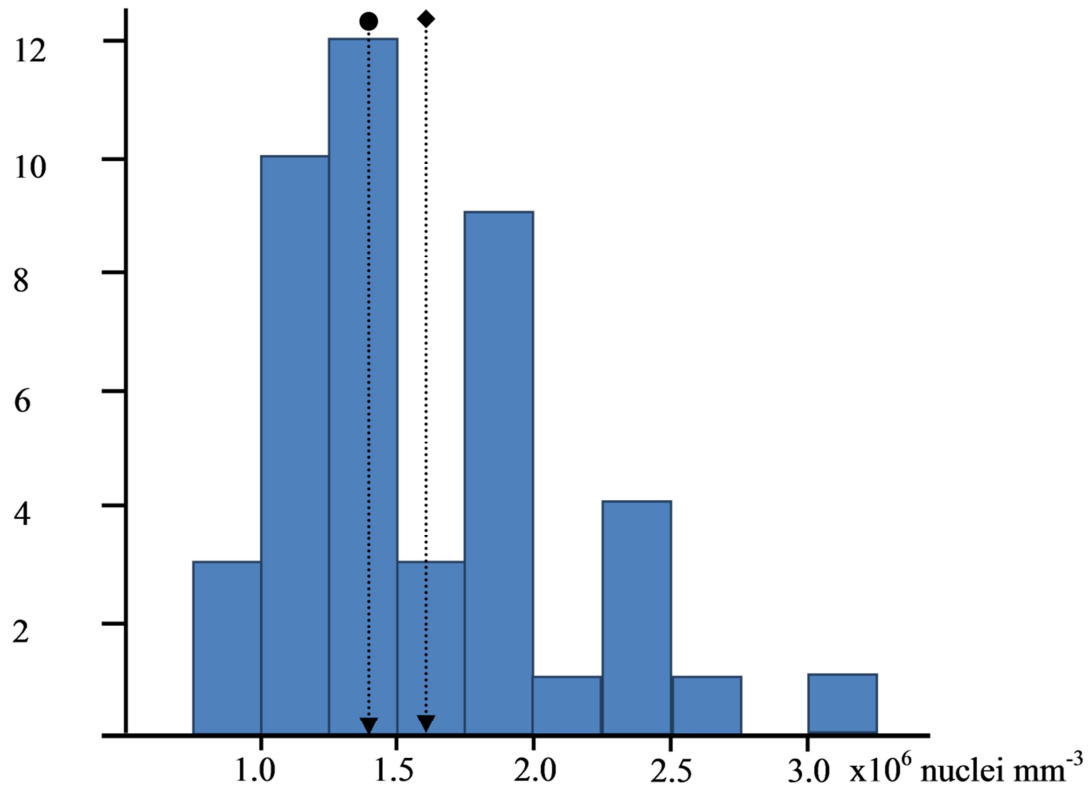
437 **Figure legends**

438



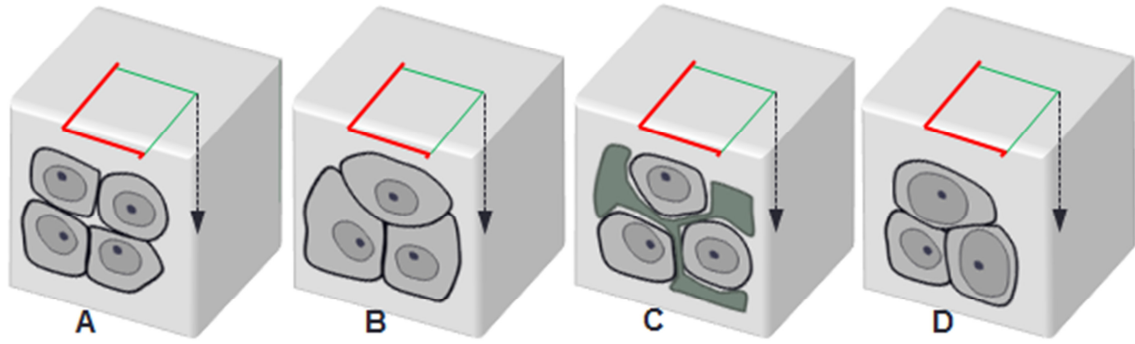
439

440 Fig. 1: Series of light micrographs from a thick section (30 μm) of a canine mammary
441 carcinoma that form an optical disector (the depth of each optical plane is indicated in
442 the upper left corner). Nuclei of neoplastic cells are counted if they are seen within the
443 counting frame or touching the inclusion (green) lines, but not touching the exclusion
444 (red) lines. In this illustrative field, 6 nuclei are counted (arrowheads); bar: 6 μm.



445
 446
 447
 448

Fig. 2: Histogram of the mean N_V (nuclei, tumor) values in the 44 canine mammary carcinomas; lozenge-arrow: mean value; circle-arrow: median value.



449
 450 Fig. 3: Potential (theoretical) explanations for the changes in the N_V (nuclei, tumor). For
 451 the sake of illustration consider a reference space (gray cube) holding particles that are
 452 counted through the optical disector (A). From B to D the N_V (nuclei, tumor) decreases
 453 through different mechanisms. In (B) cells enlarge, thus few nuclei are counted,
 454 whereas in (C) cells are apart, due to extracellular matrix deposition or loss of
 455 intercellular adhesion. In (D) cells are highly pleomorphic, some cells are considerably
 456 larger, and so few nuclei are counted in the disector.